Diffusion barrier coatings on ductile particles for protection in bioactive glass–ceramic matrix

Kwang-Leong Choy *, Ralf Balzer, Rees D. Rawlings

Department of Materials, Imperial College of Science, Technology and Medicine, Prince Consort Road, London SW7 2BP, UK

Abstract

Bioactive Apoceram glass-ceramics reinforced with ductile Ti particles are promising surgical implant materials. Unfortunately, there is a detrimental reaction between Ti particles and the Apoceram matrix leading to the formation of a brittle reaction layer of Ti_5Si_3 which prevents the attainment of the full toughening potential of the ductile particles. This paper describes the use of protective coatings on titanium particles to prevent interdiffusion, and thus to minimise the formation of the brittle reaction layer. The coating systems investigated were (i) a titanium diboride layer combined with an outer carbon layer (TiB_2/C), and (ii) a titanium boride nitride coating Ti(B,N). These coatings were deposited onto Ti particles using a magnetron sputter method prior to the incorporation into the Apoceram matrix. The structure and mechanical properties of the composites reinforced with Ti particles with and without diffusion barrier coatings were determined. It was found that the Ti(B,N) coating reduced the extent of the Ti,Si reaction layer by a factor of about 2. The coating process did not affect the particle size distribution of the titanium powder nor change the main characteristics of the crystallisation of the matrix. The coatings improved the fracture toughness and flexural strength of the composites, especially the composites reinforced with TiB_2/C coated titanium. © 2000 Published by Elsevier Science Ltd. All rights reserved.

Keywords: Bioactive materials; Diffusion barrier coatings; Glass ceramics; Ti(B,N); Ti particles

1. Introduction

A better standard of living has led to an increased life expectancy and failure of bone has become more and more frequent. To maintain the quality of life there is a need for bone substitution implant materials with a range of properties. For the substitution of load bearing bones, metallic implants are commonly used. These are commonly classified as biotolerant, i.e. there is a slight adverse reaction but this is acceptable and tolerated by the body although the implant becomes encapsulated in a non-adherent layer of fibrous tissue. Metallic implants are mechanically fixed (cemented or screwed) in the body. For lower-stress applications, e.g. ear prostheses, bioactive materials may be used. These materials are designed to induce specific biological activity that results in the formation of a strong bond with the surrounding tissue. This bond is sufficient for fixation without having to resort to cementing or screwing.[1]

The first bioactive implant materials were glasses that were developed in the seventies by Hench and co-workers.[2,3] These bioactive glasses are widely used but suffer from poor mechanical properties and, as a consequence, bioactive glass-ceramics with superior mechanical performance have been developed.

Apoceram is a bioactive glass-ceramic in the Na_2O–CaO–Al_2O_3–SiO_2–P_2O_5 system which has been developed at Imperial College.[4–6] It has a fine microstructure consisting of two crystalline phases, wollastonite ($CaSiO_3$) and apatite [$Ca_5(PO_4)_3(OH,F)$], and a small amount of residual glass. The mechanical properties of Apoceram glass-ceramics vary with composition and processing procedures but are typically in the ranges 90-180 MPa and 1.2–2.1 MPa m$^{1/2}$ for flexural strength and toughness respectively[6].

Although the mechanical performance of Apoceram and other bioactive glass-ceramics such as AW glass-ceramic developed by Kokubo and co-workers[7,8] is superior to that of glasses, further improvements are required for critical high stress applications. Consequently over the last decade there has been much interest in

* Corresponding author.
E-mail address: k.choy@ic.ac.uk (K.-L. Choy).

reinforcement of bioactive glass-ceramics. The most commonly employed reinforcements have been metals.

Biometals that may be suitable for reinforcements are Co–Cr alloys, stainless steel, silver and titanium. The effect of these metals, with the exception of silver, on the response of tissue to a bioactive glass has been investigated by Schepers, Ducheyne and De Clercq.[9] They found that stainless steel and a Co–Cr–Ni–Fe–Mo alloy disturbed the interfacial osteogenesis. In contrast, titanium did not interfere with the process of osteogenesis, which suggests that titanium is preferable as the reinforcement phase in a bioactive composite. Furthermore it has been demonstrated that Ti reinforcement results in a smaller increment in the elastic constants.[10]

Titanium has been employed for ductile particle reinforcement of Apoceram. Ti was chosen because it is an inert, biocompatible material that is widely used as an implant material. The mechanical properties of a bioactive glass-ceramic reinforced by 30 vol.%Ti have been reported.[11] The fracture toughness was 2.5 MPa m$^{1/2}$, but the strength was low at 87 ± 7 MPa. Titanium has also been employed for the ductile reinforcement of Apoceram which has typical strength and toughness values of 130 MPa and 1.85 MPa m$^{1/2}$. On reinforcement with 30%Ti the strength fell to 105 MPa and the toughness rose to 2.02 MPa m$^{1/2}$.[12,13] It was observed that during composite fabrication at elevated temperatures, the Ti reinforcement reacted with the SiO_2 in Apoceram matrix which led to the formation of a brittle reaction layer of Ti_5Si_3 which is detrimental to the mechanical performance of the composite.[12,13]

There are three possible solutions to this problem. (i) Adjust the composition of the Apoceram matrix to reduce the sintering and crystallisation temperatures and thereby restrict the extent of the reaction. This was the approach successfully adopted by Claxton and co-workers.[14–16] (ii) Use another biocompatible metal, such as silver, that does not react to the same extent with the matrix.[16] (iii) Prevent or minimise the interfacial reaction by depositing diffusion barrier coatings onto Ti particles prior to introduction into the Apoceram matrix. This last approach is reported in this paper. Two coating systems were investigated, namely a titanium diboride layer combined with an outer carbon layer (TiB_2/C) and a titanium boride nitride coating Ti(B,N). The mechanical properties of composites reinforced with titanium particles with and without diffusion barrier coatings were determined.

2. Experimental

2.1. Parent glass preparation

The procedures for the preparation of the parent glass have been described fully elsewhere[12,16] and only an outline will be given here. The parent glass (CP1) was made from the raw materials given in Table 1. With the exception of $Na_2CO_3 \cdot 10H_2O$, which was stored in a moist atmosphere to prevent efflorescence, all raw materials were dried before weighing in order to minimise errors associated with hydration. $Na_2CO_3.10H_2O$ was in the form of small crystals, hence was ground prior to mixing with the other powders in a pharmaceutical mixer which rotated in three dimensions for 1 h.

The homogeneously mixed powder was placed in a platinum crucible and the temperature was raised to 1400°C, held for 3 h and then the temperature was increased to 1500°C and held for 30 min. Finally the melt was quenched into iced water, resulting in the formation of large glass fragments. The glass fragments were subsequently powdered using a tungsten carbide Tema mill. The resulting powder was sieved to less than 38 μm.

2.2. Raw material characterisation

The titanium was supplied by Active Metals Ltd, and the quoted purity was 99.4% with a maximum oxygen content of 0.15%. A Malvern 3600 laser particle sizer was used to verify manufacturer's claim of the Ti particle size, to determine any effect of the coating process, and to establish the success of the grinding and sieving of the glass powder. The particles were suspended in distilled water and for each powder the particle size distribution was measured several times to obtain an average.

2.3. Coating of titanium powder

The coating of the titanium powder was performed using a magnetron sputtering method. The first coating system consisted of two layers; an inner layer of titanium diboride, which was deposited using a titanium diboride target and was sputtered for 4.5 h, and a second layer produced by carbon sputtering for 2.5 h. The vacuum before sputtering was typically below 5×10^{-3} torr. Subsequently, the pressure of argon gas was increased to 3×10^{-3} torr during deposition. The second coating system consisted of only a layer of Ti(B,N),

Table 1
Raw materials for the production of Apoceram of the composition CP1

Starting materials	Amount in batch (g)	Batch component
Sodium carbonate decahydrate	20.79	$Na_2O(H_2O,CO_2)$
Calcium carbonate	36.43	CaO
Alumina	6.5	Al_2O_3
Silica	51	SiO_2
Calcium orthophosphate	15.5	CaO, P_2O_5
Calcium fluoride	2.79	CaO, F

which was obtained by sputtering the titanium diboride target in an N_2 atmosphere. The thickness of both coatings was approximately 2 μm.

2.4. Composite fabrication

The optimum mechanical properties with respect to titanium volume fraction has been established by Taylor;[12,13] the highest flexural strength was obtained at 20 vol.% titanium reinforced Apoceram whereas the highest value for the fracture toughness corresponded to 30 vol.% titanium. These two titanium volume fractions were chosen for this study. The composites fabricated in this study, and their designations, are summarised in Table 2.

A mixture of Apoceram parent glass and Ti (as given in Table 2) was hot pressed in vacuum (10^{-4} torr) under a die pressure of 13 MPa. The composite was held at 1000°C for 1 h and subsequently allowed to cool in the press. This hot-pressing procedure both sintered and crystallised the matrix. The samples were in the form of discs of nominal dimensions of 38 mm diameter and 5 mm thick.

The crystallisation of the matrix was followed by the monitoring of the exothermic crystallisation peak by differential thermal analysis, DTA (Stanton Redcraft STA thermal analyser). All runs were performed using platinum crucibles in an argon atmosphere. A heating rate of 20°C/min was applied and the samples were heated from 20 to 1000°C.

2.5. Structural characterisation

X-ray diffraction (XRD) was used to determine the nature of the crystalline phases in the composites. Solid samples were scanned at 1°/min in a Philips diffractometer employing CuK radiation. Scanning electron microscopy (SEM), in both secondary and backscattered modes, was used to study the microstructures. The microscope was equipped with an energy dispersive X-ray analysis (EDX) system thus enabling quantitative chemical analysis of the interface of the matrix/reinforcement.

The amount of porosity present in the composites was determined from a comparison of the theoretical density, calculated from the law of mixtures, and experimental density as measured by Archimedes' method.

Table 2
Composites fabricated and their designations

Apoceram composite	Sample
Reinforced with 20 vol.% pure titanium	P20
Reinforced with 30 vol.% pure titanium	P30
Reinforced with 20 vol.% TiB_2/C coated titanium	C20
Reinforced with 30 vol.% TiB_2/C coated titanium	C30
Reinforced with 20 vol.% Ti(B,N) coated titanium	N20
Reinforced with 30 vol.% Ti(B,N) coated titanium	N30

2.6. Mechanical testing

The hot-pressed discs were polished on both surfaces and cut into bars using a high speed diamond saw. The ratio of the bar dimensions for three-point bending tests was 2.5: 5: 20 (B:W:S), where B was the width of bar, W was the thickness of sample (∼5 mm), and S was the distance between both supports which was ∼20 mm. Prior to testing both the tensile and compressive faces of the test bars were polished down to a 1 μm Al_2O_3 grit finish. Bars for fracture toughness testing were also notched to a depth of 0.17 W on the tensile side using a silicon disc with 400 grits. The notch had a nominal thickness of 0.15 mm.

At least three samples were tested to obtain an average value for strength and toughness. The room temperature flexural strength was determined using three-point bend test rig on a Nene M3000/64 K testing rig at a cross-head speed of 1 mm/min. The flexural strength was calculated using the equation:

$$s_f = 3PS/2BW^2 \tag{1}$$

where s_f is flexural strength, P is load at break, and B and W have been defined earlier. The plain strain fracture toughness was determined using the single edge notch bend (SENB) test in three-point bending. The notch depth was measured for each composite system using a calibrated optical microscope. The plane strain fracture toughness (K_{1c}) was calculated from experimental data using the equation:

$$K_{1c} = Y(3Ps/2BW^2)a^{0.5} \tag{2}$$

where a is notch depth and Y is a compliance factor which is given by:

$$Y = \{1.99 - a/W(1 - a/W)(2.15 - 3.39a/W$$
$$+ 2.7(a/W)^2)\}/\{(1 + 2.a/W)(1 - a/W)^{1.5}\} \tag{3}$$

and is valid for $0 < a/W < 1$ and for $s/W = 4$.[4]

Vickers hardness tests were carried out on polished surfaces in order to study the crack paths of the small cracks that emanated from the corners of the indentations. A 5 kg load was used for the Vickers hardness test.

3. Results and discussion

3.1. Characteristics of materials for composite production

Typical particle size distributions for the powders are presented in Fig. 1. The coating process had a negligible effect on the distributions for the titanium reinforcement.
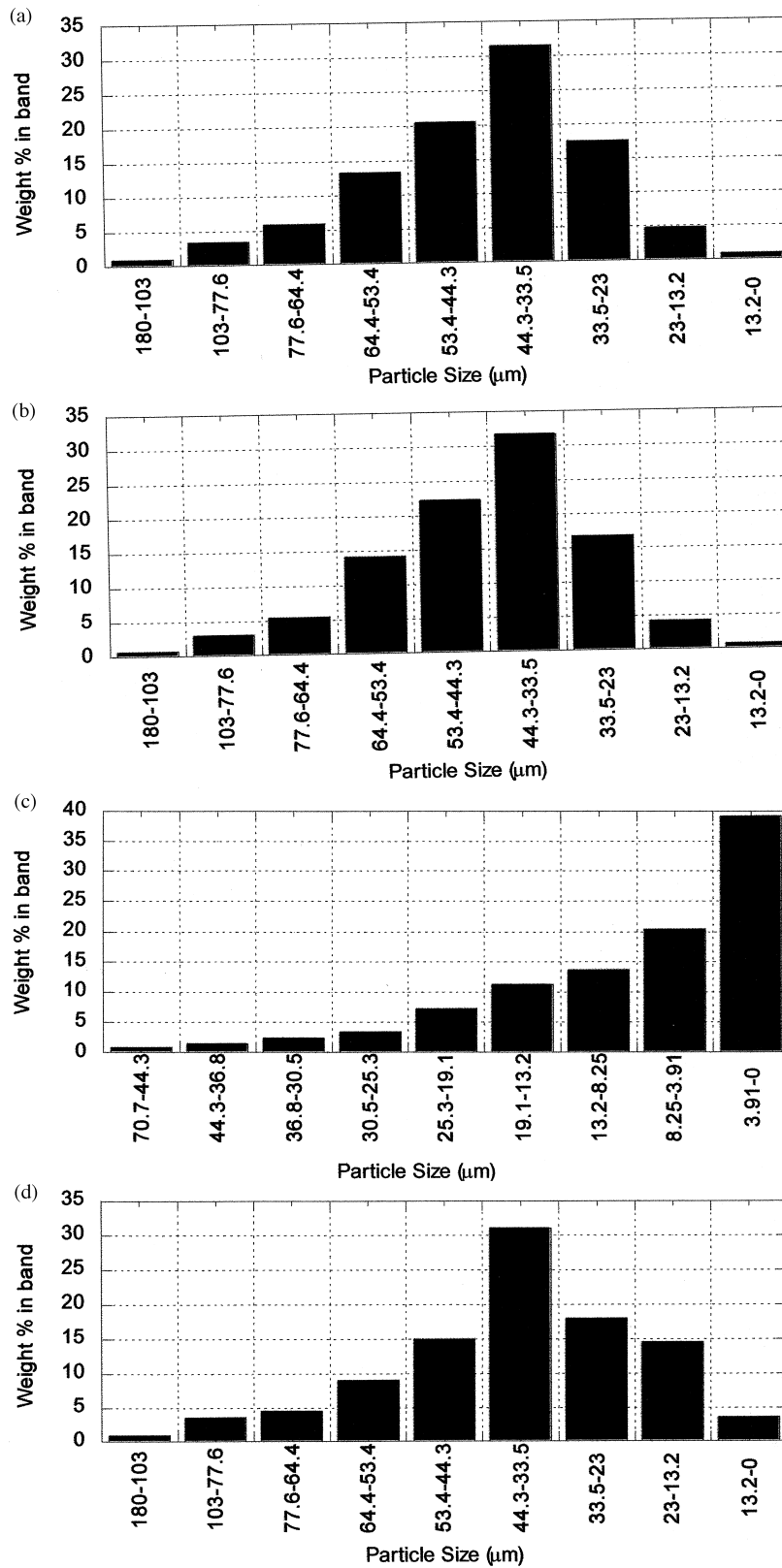
Fig. 1. Particle size distribution of the powder: (a) Ti(B,N) coated titanium; (b) TiB$_2$/C coated titanium; (c) glass; (d) Ti.

In all cases the Sauter mean particle size, D(3,2), was ~37.5 μm, with ~90% of the particles sizes in the range 23–77 μm and equal amounts (~5%) above and below this size range. In contrast the Sauter mean particle size of the glass powder was only 2.3 μm; ~90 wt.% of the particles were smaller than 23 μm, and of these ~5% were smaller than 0.6 μm.

The results obtained from particle size analysis were confirmed by SEM (Fig. 2). The micrographs also showed the glass particles to be more angular than the titanium particles.

3.2. Crystallisation and structural observations

Fig. 3 shows some typical DTA traces, all of which have two clearly distinguishable exothermic peaks. Previous work[6,9,11] has demonstrated that the first peak is due to the crystallisation of apatite and the second (larger) corresponds to the formation of wollastonite. The peaks in the traces for mixed powders (CP1 + reinforcement, i.e. P20 and C20 on the figure) are smaller because the amount of glass is lower in those samples. The peak temperatures are summarised in Table 3; those for CP1

are in good agreement with those determined by Claxton[16] and Taylor.[12] The data show that the addition of titanium did not change the crystallisation characteristics of the Apoceram matrix. This differs from the results obtained by Taylor[12] who found that although the presence of titanium had little effect on the crystallisation of apatite, it reduced the temperature of the wollastonite peak.

X-ray analysis confirmed the presence of apatite, wollastonite and titanium in the glass-ceramic matrix composites. The results indicated that the coating process did not affect the crystallisation process in the matrix, since all XRD patterns were almost identical as shown in Fig. 4, and, therefore, are consistent with the DTA data. There were some unknown peaks, but no minor phases were identified that could be attributed to an interfacial reaction. This does not, however, mean the absence of any interfacial phase as the detection limit of the XRD equipment would require several percentage by volume of a phase to be present before being detected.

A comparison of theoretical and experimental densities is given in Table 4. The theoretical data have not taken into account the presence of any interfacial phase
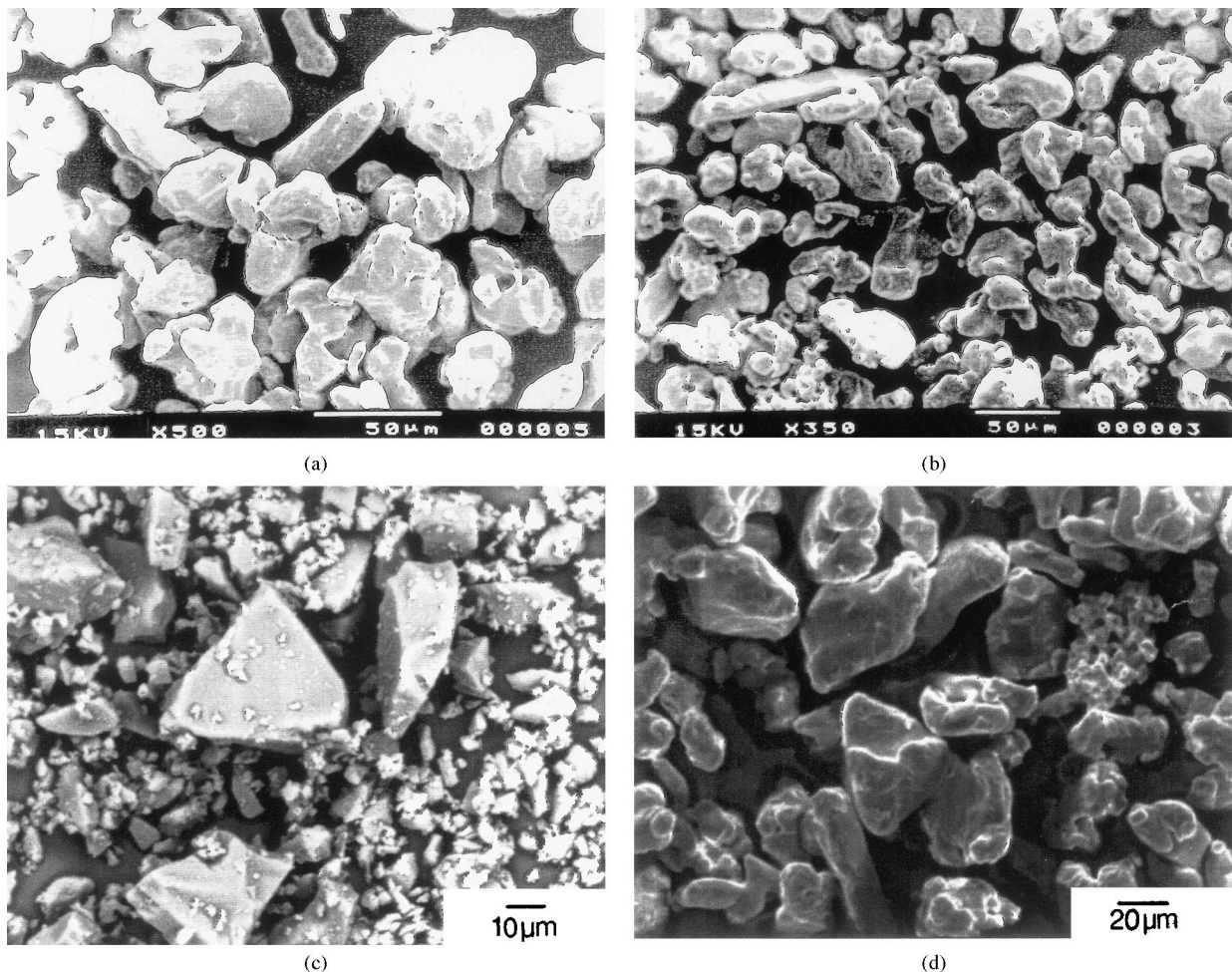

Fig. 2. Scanning electron images of the powder: (a) Ti(B,N) coated titanium; (b) TiB₂/C coated titanium; (c) glass; (d) Ti.
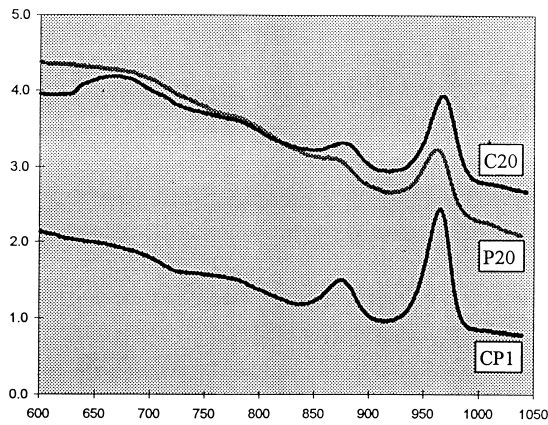
Fig. 3. Differential thermal analysis plots for powder of parent glass (CP1) and of two composites (C20 and P20).
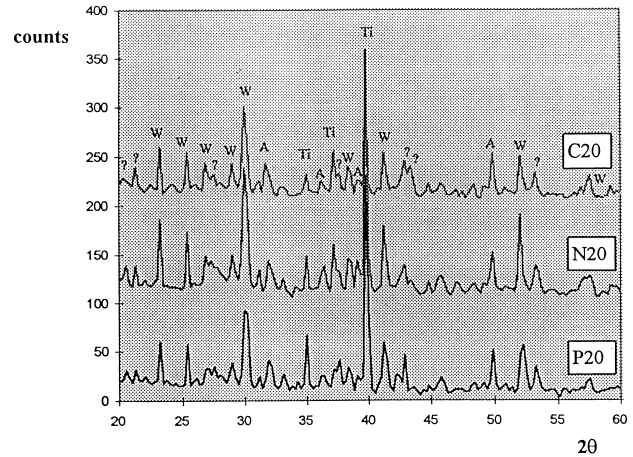

Fig. 4. X-ray diffraction showing similar patterns from three composites, C20, N20 and P20. (W, Wollastonite; A, apatite; Ti, titanium; ?, unidentified).

Table 3
Crystallisation temperature of CP1 powder (heating rate = 20°C/min)

	Crystallisation temperature apatite/°C	Crystallisation temperature Wollastonite/°C
Pure CP1	875±1°C	968±1°C
CP1 + TiB$_2$/C coated Ti	870±1°C	963±1°C
CP1 + uncoated Ti	879±1°C	968±1°C

Table 4
Densities of the composites

Material	Theoretical density, ρ_T [mg/m^3]	Measured density, ρ_M [mg/m^3]	$(\rho_M/\rho_T) \times 100$
Titanium	4.5	–	–
CP1	2.7*	–	–
P20	3.06	3.047	99.60
C20	3.06	3.052	99.74
N20	3.06	3.058	99.93

*Ref. (9).

or of variation in matrix density associated with possible changes in the matrix structure with the different reinforcements. In spite of these provisos, it may be concluded that there are only small differences between the measured and theoretical density values for the composites and that this difference decrease when coated titanium was used for reinforcing. This suggests that coating has reduced the extent of the interfacial reaction and of the accompanying porosity.

Scanning backscattered electron microscopy of etched surfaces of the composites showed the microstructure of the matrix, remote from the interface with the titanium particles, to be similar to that reported for monolithic Apoceram prepared under the same hot pressing conditions,[6] namely a fine (crystal length typically 10 μm) intimate dispersion of crystals in a matrix of residual glass (Fig. 5).

Micrographs from unetched surfaces showed an interfacial reaction and porosity in all of the composites (see for example the micrograph for C30 of Fig. 6). It was not possible to draw any conclusions as to the extent of the interfacial reaction from the scanning electron micrographs. Three different types of pores were identified: (i) within the matrix, (ii) in the matrix close to the reaction layer, and (iii) in the titanium particles close to the reaction layer.

The pores within the matrix may have been associated with the density change from the glass to crystalline phases but more likely were due to poor sintering; it is well established that the presence of rigid reinforcement particles develop localised strains in the matrix that hinder sintering[17–19] and ductile metal reinforcement particles would probably have a similar effect.

The pores close to the interface could have originated through differences in thermal expansion coefficients between the reinforcement and the matrix, the Kirkendall effect (rapid diffusion of a species by vacancy mechanism) or the generation of a gaseous species (oxygen) during composite fabrication at elevated temperatures (>700°C) under vacuum according to the equation:

$$5Ti(metal) + 3SiO_2(glass) \ \rightarrow \ Ti_5Si_3(interface) + 3O_2$$

$$(4)$$
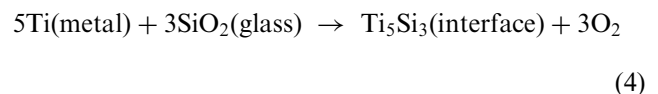
The Kirkendall effect and generation of oxygen are consider to be the most probable mechanisms.

EDX elemental mapping of the interfacial region was conducted on sample N20 and compared with the results of a similar analysis reported by Taylor[12] for P20. Fig. 7a shows the phase map of the interface and Fig. 7b is the corresponding backscattered electron
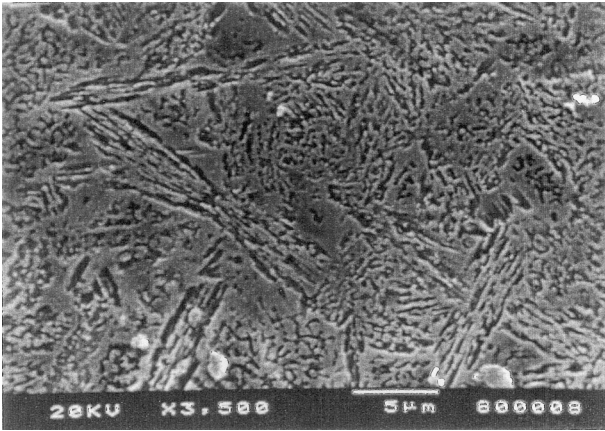
Fig. 5. Microstructure of the etched matrix of composite P20 remote from the titanium reinforcement.
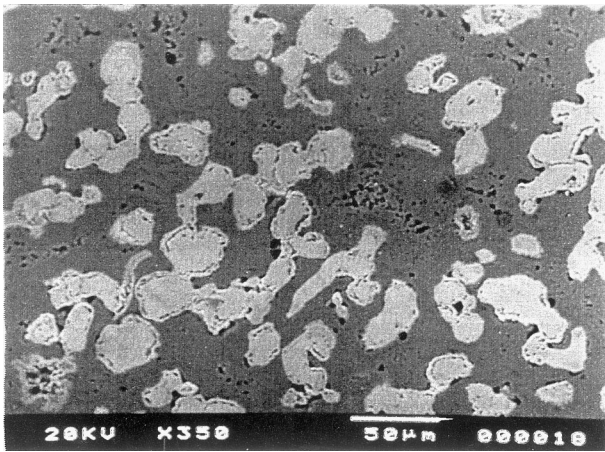

Fig. 6. Backscattered electron micrographs of unetched composite C30 showing type and distribution of flaws.

micrograph; the crosses mark the same point on the sample. Note that EDX is not capable of detecting light elements such as nitrogen and boron, therefore the coating was not located. It is clear that the coating on the Ti did not prevent the formation of a Ti/Si reaction layer as the grey region around the Ti particle (lighter coloured green) indicated the formation of titanium silicide. However, the coating had restricted the thickness of the reaction layer to 2 μm compared with 4 μm in the uncoated Ti reinforced Apoceram (Fig. 8). Adjacent to the Ti/Si layer, there is a very thin layer (coloured white) consisting of Ti, Si and Al. The light grey regions correspond to wollastonite, $CaSiO_3$. The associated darker surrounding regions contain Ca, Si and Al but no Ti. There is a region of thickness of about 2 μm surrounding the reaction layer which is wollastonite free.

It is difficult to unambiguously locate the original reinforcement-matrix interface and to allocate formation mechanisms for the different types of pores. However, the porosity throughout the titanium silicide layer is characteristic of Kirkendall porosity resulting from different diffusion rates for titanium and silicon. The porosity situated at the interface between the titanium silicide interfacial layer and the wollastonite-free layer consists of a large number of small, approximately spherical pores which have linked. A similar form of porosity has been reported in SiC reinforced "Silceram" glass-ceramic due to the formation of a gaseous species by an oxidative reaction.[20] This porosity in the present composites is therefore attributed to the oxygen produced by the reaction given in Eq. (4).

The continuous "porosity" close to the boundary between the wollastonite-free layer and the matrix may in fact be cracking. Thermal stresses will be developed
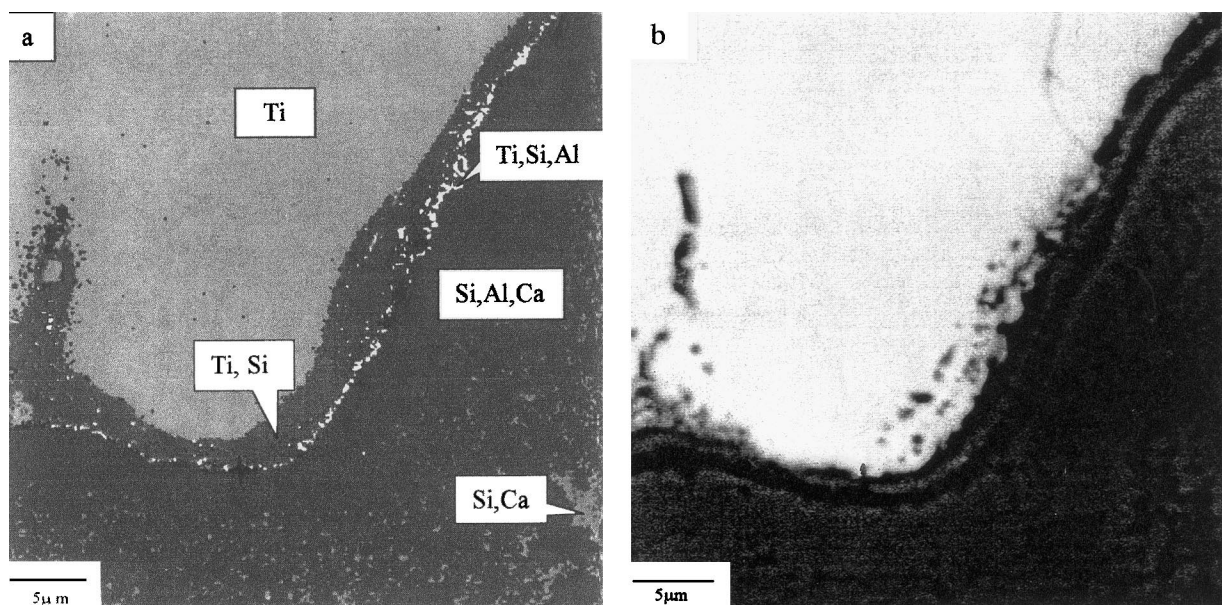

Fig. 7. Interfaces of Ti(B,N) coated Ti reinforced Apoceram composite (N20): (a) phase map and (b) backscattered electron image.

due to differences in expansion coefficients of the matrix and reinforcement materials. However, the relative values for the coefficients, namely 8.6×10^{-6} and $\sim 11 \times 10^{-6}$ K^{-1} for titanium and Apoceram respectively, would lead to hoop tension and thus radial cracking and not to the observed circumferential cracking. It is concluded that this undesirable artifact is not due to thermal coefficient differences between the reinforcement and matrix but must be related in some way to the change from a wollastonite-free structure to the normal matrix structure. Stresses accompanying crystallisation can cause cracking in glass-ceramics, so a possibility is that cracking occurs in the weaker wollastonite-free layer due to the stresses developed by the crystallisation of wollastonite in the neighbouring matrix.

3.3. Mechanical properties

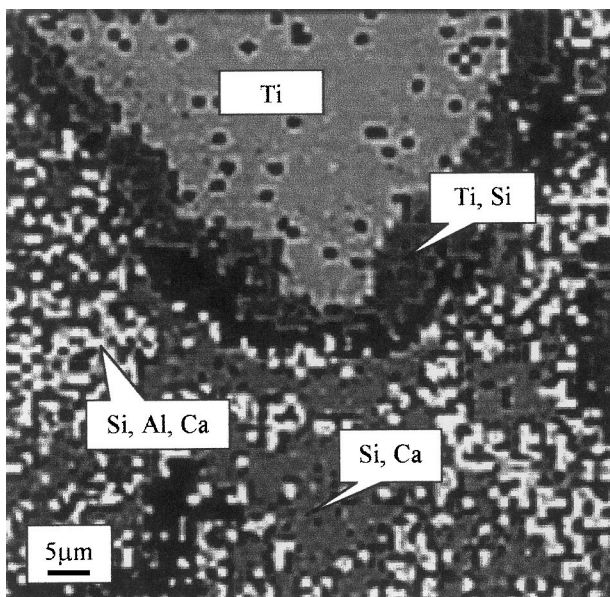The results of the three-point bend strength and single-edge notched beam fracture tests for coated Apoceram-titanium composites with 20 vol.% reinforcement are summarised, normalised to the uncoated system, in Fig. 9. With the exception of N20, the fracture toughness of the composites with coated particles was greater than that of the composites of the same volume fraction of uncoated particles. In addition, all the coated systems exhibited superior strength to their uncoated counterparts. A similar trend was observed in the coated Apoceram-titanium composites with 30 vol.% reinforcement.

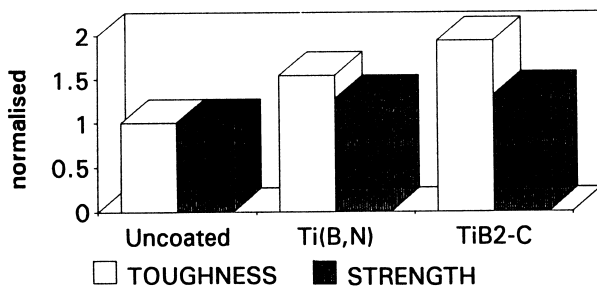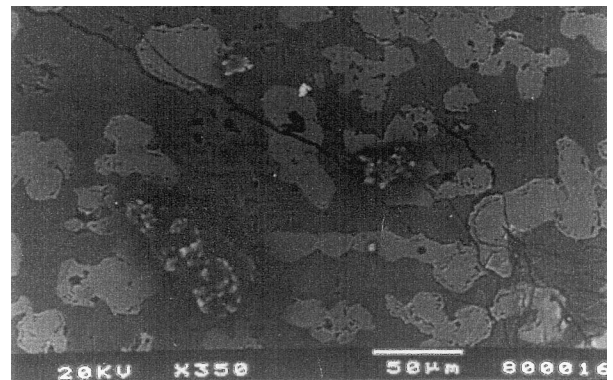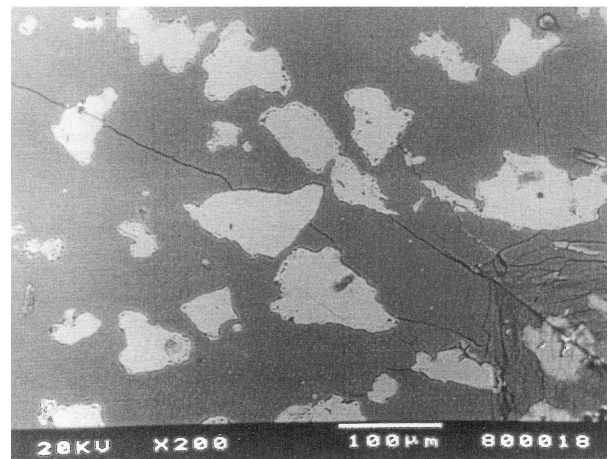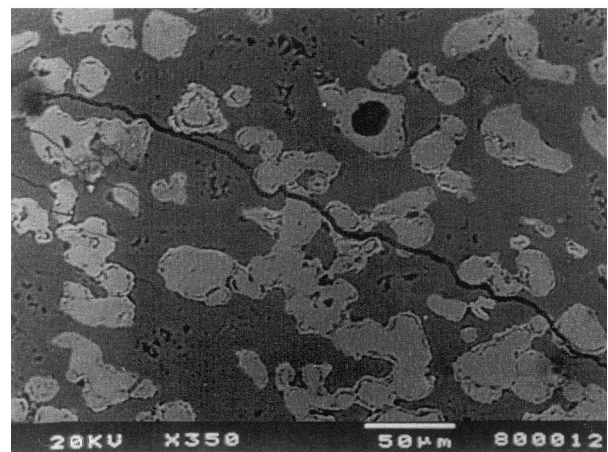Fig. 8. A phase map showing interfaces of uncoated Ti reinforced Apoceram composite (P20).[13]

Fig. 9. Comparison of the mechanical properties of the various Apoceram–titanium composites (20 vol.% reinforcement).

Fig. 10. Crack path in the composites: (a) N30; (b) P20; (c) C30.

As discussed earlier the difference in expansion coefficients leads to hoop tension in the matrix around a titanium particle and consequently a propagating crack will be attracted towards the particle. There are then three possibilities once the crack reaches a particle: (i) the crack propagates through the particle with little plastic deformation, (ii) a limited amount of debonding occurs and the particle deforms, and (iii) the crack is deflected along a weak matrix-reinforcement interface. Possibility (ii), which requires an intermediate interfacial strength and a ductile particle, is the most desirable for a good mechanical performance but was rarely observed in the present work. The most commonly observed fracture path was deflection around the particles although propagation through the particles with negligible plastic deformation also occurred in the uncoated and Ti(B,N) coated titanium containing composites (Fig. 10). This demonstrates that the TiB_2/C coating gives a reproducible, low strength interface. In contrast, the presence of the two crack paths in the other composites suggests that the interface is of more variable quality, and hence variable strength. An explanation for the lack of plastic deformation of a metallic particle when a crack passes through it is that the interface is sufficiently strong to cause a high degree of constraint and hence a small crack opening displacement. This may be the reason for the lack of deformation of the titanium particles but a contributing factor may also be the embrittlement of the titanium by oxygen in solution.

4. Conclusions

The coating process did not affect the particle size distribution of the titanium powder nor change the main characteristics of the crystallisation of the matrix.

The coatings improved the fracture toughness and flexural strength of the composites, especially the composites reinforced with TiB_2/C coated titanium. In most cases the cracks were deflected along the particle-matrix interface although in the composites with uncoated and Ti(B,N) coated titanium the crack sometimes propagatedthrough the particles with negligible plastic deformation.

It was found that the Ti(B,N) coating reduced the extent of the Ti,Si reaction layer by a factor of about 2.

There was also a wollastonite-free layer (approximately 5 μm thick) in the matrix adjacent to Ti,Si reaction layer.

Acknowledgements

References

1. Rawlings, R. D., *Clin. Mater.*, 1993, **14**, 155–179.
2. Hench, L. L. and Paschall, H. A. J., *Biomed. Mater. Res. Symp.*, 1973, **4**, 25–42.
3. Hench, L. L., Splinter, R. J., Allen, W. C. and Greenlee, T. K. J., *Biomed. Mater. Res.*, 1972, **2**, 117–141.
4. Carpenter, P. R., Cambell, M., Rawlings, R. D. and Rogers, P. S. J., *Mater. Sci. Lett.*, 1986, **5**, 1309–1312.
5. Rawlings, R. D., Rogers, P. S. and Stokes, P. M., In *High Tech Ceramics*, ed. P. Vincenzini. Elsevier Science Publishers, B.V. Amsterdam, 1987, pp. 73–82.
6. Alanyali, H., Rawlings, R. D. and Rogers, P. S., *Br. Ceram. Trans.*, 1998, **97**, 240–245.
7. Kokubo, T., Shigematsu, M., Nagashima, Y., Tashiro, M., Nakamura, T., Yamamuro, T. and Higashi, S., *Bull. Inst. Chem. Res., Kyoto University*, 1982, **60**, 260–268.
8. Kokubo, T., Ito, S., Sakka, S. and Yamamuro, T., *J. Mater. Sci.*, 1986, **21**, 536–540.
9. Schepers, E., Ducheyne, P. and De Clercq, M., *J. Biomed. Mater. Res.*, 1989, **23**, 735–752.
10. Pernot, F. and Rogier, R., *Bioceramics,* ed. G. Heimke, German Ceramic Soc., 1990, Vol. 2, pp. 311–320.
11. Troczynski, T. B. and Nicholson, P. S., *J. Am. Ceram. Soc.*, 1991, **74**, 1803–1806.
12. Taylor, B., PhD thesis, Imperial College, London University, 1995.
13. Taylor, B., Rawlings, R. D., Rogers, P. S., *Bioceramics*, ed. O. H. Andersson and A. Yli-Urpo, Butterworth-Heinemann, 1994, Vol. 7, pp. 255–260.
14. Claxton, E., Rawlings, R. D. and Rogers, P. S., In *Brit. Ceram. Proc.*, ed. D. P. Thompson and H. Mandal. Inst. Mater., 1996, No. 55, 101–112.
15. Claxton, E., Rawlings, R. D. and Rogers, P. S., Proc. 7th Europ. Conf. On Composite Materials, Woodhead Publishing, Cambridge, 1996, Vol. 2, pp. 461–465.
16. Claxton, E., PhD thesis, Imperial College, London University, 1996.
17. Sudre, O. and Lange, F. F., *J. Am. Ceram. Soc.*, 1992, 75, 519–524.
18. Sudre, O. Bao, G. Fan, B. and Lange, F. F., *J. Am. Ceram. Soc.*, 1992, 75, 525.
19. Lange, F. F. J., *Mater. Res.*, 1987, **2**, 59–65.
20. Saewong, P., PhD thesis, Imperial College, London University, 1998.